Multi-Dimensional, Wide-Range, and Modulation-Format-Transparent Transceiver Imbalance Monitoring

Qun Zhang, Yanfu Yang, Chao Gu, Yong Yao, Alan Pak Tao Lau, and Chao Lu

***Abstract*—We propose and experimentally demonstrate a dual-polarization (DP) transceiver imbalance monitoring scheme, which is applicable for the coherent system using square QAM signals. The scheme can separate/monitor various kinds of transceiver imbalances and has technical advantages of multi-dimension, wide monitoring range, and modulation-format-transparency. In the proposed scheme, a polarization scrambler is configured between transmitter (Tx) and receiver (Rx). After coherent detection, the proposed digital signal processing (DSP) modules are implemented to monitor transceiver imbalance based on the received signals. To simplify the DSP modules, the implementation sequence of DSP modules is in reverse order compared to the order in which the sequence of impairments is introduced. Firstly, Godard timing error detection (TED) and Gram-Schmidt orthogonalization procedure (GSOP) is used to monitor and compensate Rx imbalances. After compensating the Rx imbalances, Tx imbalance monitoring is implemented. Complex/real maximum likelihood independent component analysis (ML-ICA) and Godard-TED are used to monitor Tx imbalance. Finally, the amplitude ratios of the final output signal and Tx in-phase/quadrature (IQ) amplitude imbalance are fed back to mitigate the interaction of Tx imbalances on the signal power and improve monitoring accuracy. The transceiver IQ and x-polarization/y-polarization (XY) imbalances are separated for the first time by using the frequency offset (FO) naturally existing in the system and the continuous polarization rotation induced by a polarization scrambler. The separation method combined with the reverse algorithm design and amplitude ratio feedback mechanism makes the proposed scheme achieve the most multi-dimensional imbalance monitoring by far. The simulation and experimental results verify that the proposed scheme is modulation-format-transparent and can separate/monitor multi-dimensional transceiver imbalances within a wide range.**

***Index Terms*—Optical fiber communication, digital signal processing, parameter estimation, communication system fault diagnosis.**

I. Introduction

The increasing bandwidth demand of optical communication is driven continually by the rapid growth of global Internet traffic. In order to meet the demand, the increase of transmission rate and modulation format order has become an inevitable trend of optical communication development. However, high symbol rate and high modulation order signal transmission is vulnerable to receiver (Rx) and transmitter (Tx) imbalances. Therefore, the transceiver imbalance monitoring technology is indispensable for ensuring a reliable communication system. Compared with direct detection system, the coherent detection system employs more complex optoelectronic devices and has more parameters that need to be monitored, which imposes higher requirement on the monitoring technology. To be specific, the monitoring scheme should be able to separate and estimate various imbalances with strong noise robustness and wide monitoring range. In addition, considering multiple modulation formats may be adaptively configured in the future elastic optical network, the modulation-format-transparent feature is very crucial. Therefore, the expected imbalance monitoring scheme should have the characteristics of multi-dimension, robustness, wide range, and modulation-format-transparency.

In the dual-polarization (DP)-transceiver of a coherent optical communication system, the device imbalances can be divided into in-phase/quadrature (IQ) and x-polarization/y-polarization (XY) imbalances according to the reference dimension, and divided into amplitude/phase imbalance and time skew according to the imbalance type. At Tx side, the amplitude imbalance is caused by the mismatch of the driving amplifier gain and the optical coupler coupling ratio; the phase imbalance is induced by the improper configuration of $\pi/2$ phase shift related bias voltage; the time skew is mainly caused by the different lengths between optical and electrical paths. At Rx side, the amplitude is mainly induced by the mismatch between the output power of balanced detector and the gain of

This work was supported by the Shenzhen Municipal Science and Technology Plan Project (JCYJ20190806142407195) and National Key R&D Program of China Project (2019YFB1803502). (*Corresponding Authors: Yanfu Yang.*)

Q. Zhang, Y. Yang, C. Gu, and Y. Yao are with the Department of Electronic and Information Engineering, Harbin Institute of Technology, Shenzhen, China. (e-mail: 16b958076@stu.hit.edu.cn; 18s052075@stu.hit.edu.cn; yangyanfu@hit.edu.cn; yaoyong@hit.edu.cn).

C. Lu is with the Department of Electronic and Information Engineering, Hong Kong Polytechnic University, Hung Hom, Kowloon, Hong Kong, China (e-mail: chao.lu@polyu.edu.hk).

A. P. T. Lau is with the Department of Electrical Engineering, Hong Kong Polytechnic University, Hung Hom, Kowloon, Hong Kong, China. He is also with The Hong Kong Polytechnic University Shenzhen Research Institute, Shenzhen 518057, China (e-mail: eeaptlau@polyu.edu.hk).

transimpedance amplifier (TIA); the phase imbalance is caused by the phase imperfection of optical hybrid; the time skew is also caused by the length mismatch between different optical/electrical paths [1]-[3].

To this end, although the compensation scheme of transceiver imbalance has been comprehensively investigated [1],[3]-[6], there are relatively few transceiver imbalance monitoring schemes. Gram-Schmidt orthogonalization procedure (GSOP) [4] and Löwdin orthogonalization procedure (LOP) [5] are two common compensation algorithms of amplitude/phase imbalance and all these algorithms are based on statistical analysis principle. The orthogonalization matrix obtained by these algorithms can be further used to estimate amplitude/phase imbalance [7]-[8]. Among them, GSOP is an asymmetrical orthogonalization scheme with lower complexity but will amplify the quantization noise; while LOP is based on symmetric orthogonalization with higher complexity and is robust to quantization noise [5]. Godard and square law nonlinearity (SLN) timing error detection (TED) can be used to estimate time skew in the frequency domain. Godard-TED requires two samples per symbol and can extract time skew from the autocorrelation coefficient of the spectrum of received signals at 1/2T (T is symbol period) [9]. SLN-TED requires four samples per symbol and can extract time skew from the spectrum of the squared signal at 1/T [10]. Due to the required fewer samples, Godard-TED has lower complexity compared with SLN-TED. The multiple-input and multiple-output (MIMO) equalizer using finite impulse response (FIR) filter can be used to jointly compensate amplitude/phase imbalance and time skew [3],[11]-[12]. Subsequently, the coefficients of the converged FIR filter can be used to estimate these imbalances [13]-[14]. However, the conventional MIMO equalizers, such as constant modulus algorithm (CMA) [11]-[12], radius directed equalization (RDE) [12], and decision-directed least mean square (DD-LMS) [3], are modulation-format-dependent, suffer from the singularity, and have a degraded performance under too low or high signal-to-noise ratio (OSNR) condition without training data.

The above schemes can be used to monitor Rx imbalance directly or monitor Tx imbalance without Rx imbalance, polarization crosstalk, and carrier phase recovery noise. Besides, some special Tx imbalances algorithms using extra detection devices are investigated [15]. However, there are some technical issues that should be solved to achieve transceiver imbalance monitoring for future elastics optical networks: 1) the separation issue between Tx and Rx imbalances. When the imbalances exist in both Tx and Rx, the conventional schemes can not distinguish these imbalances successfully and fail to estimate imbalance parameters; 2) narrow monitoring range. This is caused by the poor robustness of ASE noise and Tx imbalance; The conventional schemes are not robust to ASE noise and its performance is not clear in a wide OSNR range. Besides, the reported polarization tracking and carrier phase recovery (CPR) schemes have poor tolerance against Tx imbalance and will be degraded in presence of Tx imbalance. Considering the Tx imbalance monitoring is implement after the polarization tracking and CPR, this will degrade the performance of the subsequent Tx imbalance monitoring [16]; 3) Modulation-format-dependence. There is no modulation-format-transparent scheme for transceiver imbalance monitoring at present, which makes the performance monitoring of elastic optical networks difficult to achieve.

To separate Tx and Rx imbalances, various transceiver IQ imbalance monitoring schemes dependent on frequency offset (FO) have been proposed [17]-[20]. These schemes can monitor Rx and Tx imbalances before and after FO compensation, respectively. Liang et al. uses GSOP and MIMO algorithms to estimate transceiver IQ amplitude/phase imbalance and skew [19]; our previous research utilizes the convex hull assisted ellipse correction and k-means clustering assisted blind phase search scheme to monitor transceiver IQ amplitude/phase imbalance [17]. However, these existing schemes can only separate the transceiver IQ imbalances and are unable to separate the transceiver XY imbalances. In particular, Skvortcov et al. indicates polarization rotation can be used to separate transceiver XY skew [20]. Tx XY skew can be estimated by sweeping XY skew at Tx side, which is immune to Rx XY skew. However, the training data sets with different Tx XY skew should be transmitted before Tx XY skew monitoring. Therefore, the scheme is only applicable to off-line signal processing, the accuracy depends on training data. To increase monitoring range and achieve modulation-format-transparency, we have proposed a Tx IQ imbalance estimation algorithm based on maximum likelihood independent component analysis (ML-ICA) in the previous research [16]. In the scheme, complex and real ML-ICA algorithms are used to implement polarization tracking and CPR, respectively. Furthermore, the Tx IQ amplitude/phase imbalance can be estimated from the inverse IQ mixed matrix obtained by real ML-ICA. The experimental results verify that the scheme has a wide monitoring range for PDM-QPSK/8QAM/16QAM/64QAM signals. However, the ML-ICA fails to converge when FO exists due to the use of a complex score function. Therefore, the scheme is not applicable in presence of FO and is not capable of transceiver IQ imbalance separation based on FO. Besides, the scheme can not estimate time skew and the monitoring dimension is limited.

In this paper, we proposed a novel DP-transceiver imbalance monitoring scheme by upgrading our previously proposed Tx IQ imbalance estimation algorithm [16]. This scheme is applicable for the coherent detection system using square QAM signals and can separate and monitor transceiver IQ and XY imbalances. The transceiver impairments that can be monitored including: Tx/Rx IQ amplitude imbalance, phase imbalance, and skew; Tx/Rx XY amplitude imbalance and skew. The FO naturally existing in the system and continuous polarization rotation induced by polarization scrambler are utilized to separate transceiver IQ and XY imbalances, respectively. To facilitate the implementation of transceiver IQ imbalance separation based on FO, a modified complex ML-ICA with the real score function is used to implement FO-immune polarization tracking. GSOP and Godard-TED algorithms are introduced to increase monitoring dimension. The simulation results show that the scheme can achieve reliable separation and

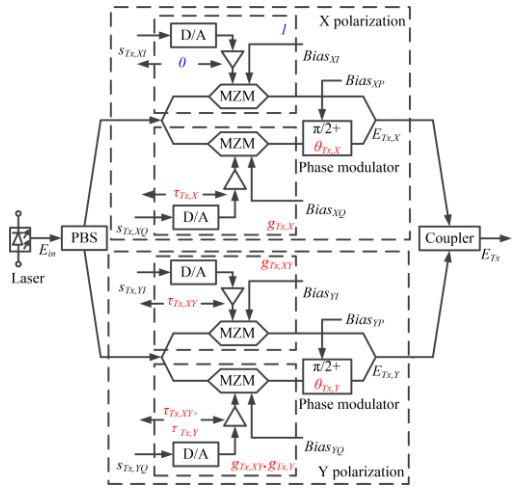

Fig. 1 Tx model. PBS: polarization beam splitter; D/A: digital-to-analog conversion circuit; MZM: Mach-Zehnder modulator; *Bias*: direct-current bias voltage.

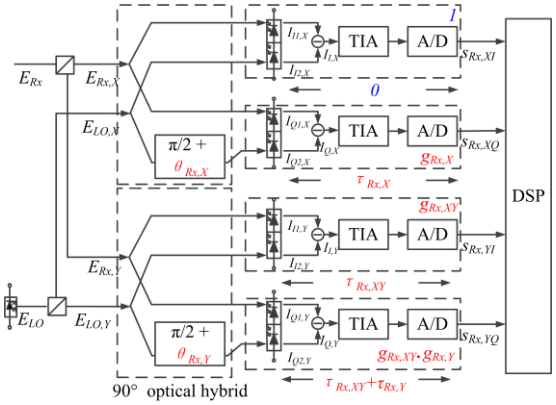

Fig. 2 Rx model. A/D: analog-to-digital conversion circuit.

estimation of transceiver imbalances within a wide range compared with complex-RDE/extend Kalman filter (EKF)/DDLMS. The PDM-QPSK/16QAM/64QAM experimental results demonstrate that the scheme can achieve multi-dimensional and modulation-format-transparent transceiver imbalance monitoring over a wide monitoring range.

The remainders of the paper are as follows: in section II, the system model under imbalance impairments is given firstly. Subsequently, the detailed principles of imbalance monitoring are given, including Rx imbalance monitoring, Rx and Tx imbalances separation, and Tx imbalance monitoring. Among them, Rx and Tx imbalances separation is verified by the comparison between the single Rx imbalance monitoring and Rx imbalance monitoring under Tx imbalance. In section III, the numerical simulation is implemented. The impacts of imbalances interaction on each imbalance monitoring are discussed firstly. Then the proposed scheme is compared with DDLMS/EKF/RDE algorithm to verify the wide monitoring range. In section IV, the proposed scheme is experimentally verified using PDM-QPSK/16QAM/64QAM signals. In section V, the conclusion is presented.

II. Principle of Imbalance Separation and Monitoring

The general mathematical models of back-to-back (BTB) system under imbalance impairments are given in this section, including Tx, link, and Rx models. Then, the DSP flow and the detailed principle of imbalance separation and monitoring is presented successively.

A. System model

The transceiver consists of Rx and Tx and the related mathematical models with device imbalances are given in this section. Device imbalances include Tx/Rx IQ and XY imbalance. Among them, $g_{Tx/Rx,X/Y}$, $\theta_{Tx/Rx,X/Y}$, and $\tau_{Tx/Rx,X/Y}$ represent Tx/Rx IQ amplitude imbalance, phase imbalance, and skew on X/Y polarization, respectively; $g_{Tx/Rx,XY}$ and $\tau_{Tx/Rx,XY}$ represent XY amplitude imbalance and skew at Tx/Rx side, respectively.

A typical DP-Tx configuration is shown in Fig. 1. Assuming the ideal transmitted signal is $s_{Tx,mn}(n)$, where *mn* can be one of {*XI*, *XQ*, *YI*, *YQ* } and represents four components of DP-IQ modulated signal. Given that the MZM modulator operates in the linear region, the baseband transmitted signal can be expressed as [9],[21]:

$$\begin{bmatrix} s'_{Tx,XI}(t) \\ s'_{Tx,XQ}(t) \end{bmatrix} = \begin{bmatrix} 1 & -g_{Tx,X}\sin(\theta_{Tx,X}) \\ 0 & g_{Tx,X}\cos(\theta_{Tx,X}) \end{bmatrix} \begin{bmatrix} 1 & 0 \\ 0 & \delta(t_s-\tau_{Tx,X}) \end{bmatrix} \otimes \begin{bmatrix} s_{Tx,XI}(t) \\ s_{Tx,XQ}(t) \end{bmatrix} \tag{1}$$

$$\begin{bmatrix} s'_{Tx,YI}(t) \\ s'_{Tx,YQ}(t) \end{bmatrix} = \begin{bmatrix} g_{Tx,XY} & -g_{Tx,XY}g_{Tx,Y}\sin(\theta_{Tx,Y}) \\ 0 & g_{Tx,XY}g_{Tx,Y}\cos(\theta_{Tx,Y}) \end{bmatrix} \begin{bmatrix} \delta(t-\tau_{Tx,XY}) & 0 \\ 0 & \delta(t-\tau_{Tx,XY}-\tau_{Tx,Y}) \end{bmatrix} \otimes \begin{bmatrix} s_{Tx,YI}(t) \\ s_{Tx,YQ}(t) \end{bmatrix} \tag{2}$$

where $\otimes$, *n*, and T_s represent the convolution operation, signal index, and sample period. It is noteworthy that (1) and (2) represent the transmitted signal models on X and Y polarization. The difference between (1) and (2) is caused by XY amplitude imbalance and skew.

Then the modulated optical signal at Tx side can be expressed as:

$$E_{Tx} = \begin{bmatrix} E_{Tx,X}(t) \\ E_{Tx,Y}(t) \end{bmatrix} = \begin{bmatrix} E_{Tx,XI}(t)+iE_{Tx,XQ}(t) \\ E_{Tx,YI}(t)+iE_{Tx,YQ}(t) \end{bmatrix} \propto \begin{bmatrix} s'_{Tx,XI}(t)+is'_{Tx,XQ}(t) \\ s'_{Tx,YI}(t)+is'_{Tx,YQ}(t) \end{bmatrix} \exp(j\omega_s t) \tag{3}$$

where ω_s is the central frequency of transmitted laser.

If ignoring ASE noise, the main link impairment between Rx and Tx in the BTB system is polarization misalignment. The received optical signal can be expressed as:

$$E_{Rx}(t) = \begin{bmatrix} E_{Rx,X}(t) \\ E_{Rx,Y}(t) \end{bmatrix} \propto \boldsymbol{J_R}(t)E_{Tx}(t) = \begin{bmatrix} \cos(\kappa(t))\exp(i\xi(t)) & -\sin(\kappa(t))\exp(i\eta(t)) \\ \sin(\kappa(t))\exp(-i\eta(t)) & \cos(\kappa(t))\exp(i\xi(t)) \end{bmatrix} \begin{bmatrix} E_{Tx,X}(t) \\ E_{Tx,Y}(t) \end{bmatrix} \tag{4}$$

where $\boldsymbol{J_R}$ represents Jones matrix (polarization misalignment

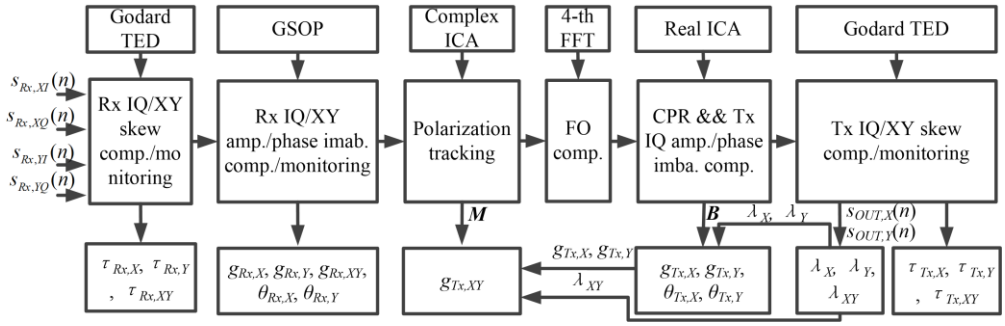

Fig. 3 DPS flow of transceiver imbalance monitoring.

or polarization rotation matrix), κ represents the azimuth angle between the fast axis and slow axis of fiber, ξ and η represent the polarization-dependent phase [22].

A typical DP-Rx model with imbalance impairments is shown in Fig. 2, where E_{LO} is the local oscillation (LO) laser and can be expressed as:

$$E_{LO} \propto \exp(j\omega_{LO}t) \tag{5}$$

Amusing the ideal received signals are as follows:

$$\begin{bmatrix} s_{XI}(t) \\ s_{XQ}(t) \end{bmatrix} \propto \begin{bmatrix} \Re e(E_{Rx,X}(t)E_{LO,X}^{*}(t)) \\ \Im m(E_{Rx,X}(t)E_{LO,X}^{*}(t)) \end{bmatrix} \tag{6}$$

$$\begin{bmatrix} s_{YI}(t) \\ s_{YQ}(t) \end{bmatrix} \propto \begin{bmatrix} \Re e(E_{Rx,Y}(t)E_{LO,Y}^{*}(t)) \\ \Im m(E_{Rx,Y}(t)E_{LO,Y}^{*}(t)) \end{bmatrix} \tag{7}$$

Then the received signals with Rx imbalance can be expressed as:

$$\begin{aligned} \begin{bmatrix} s_{Rx,XI}(t) \\ s_{Rx,XQ}(t) \end{bmatrix} &\propto \begin{bmatrix} 1 & 0 \\ 0 & \delta(t-\tau_{Rx,X}) \end{bmatrix} \\ &\otimes \begin{bmatrix} 1 & 0 \\ -g_{Rx,X}\sin(\theta_{Rx,X}) & g_{Rx,X}\cos(\theta_{Rx,X}) \end{bmatrix} \begin{bmatrix} s_{XI}(t) \\ s_{XQ}(t) \end{bmatrix} \end{aligned} \tag{8}$$

$$\begin{aligned} \begin{bmatrix} s_{Rx,YI}(t) \\ s_{Rx,YQ}(t) \end{bmatrix} &\propto \begin{bmatrix} \delta(t-\tau_{Rx,XY}) & 0 \\ 0 & \delta(t-\tau_{Rx,XY}-\tau_{Rx,Y}) \end{bmatrix} \\ &\otimes \begin{bmatrix} g_{Rx,XY} & 0 \\ -g_{Rx,XY}g_{Rx,Y}\sin(\theta_{Rx,Y}) & g_{Rx,XY}g_{Rx,Y}\cos(\theta_{Rx,Y}) \end{bmatrix} \begin{bmatrix} s_{YI}(t) \\ s_{YQ}(t) \end{bmatrix} \end{aligned} \tag{9}$$

B. The algorithm flow of transceiver imbalance monitoring

The DSP flow is shown in Fig. 3, where M and B represent inverse Jones matrix obtained by complex ML-ICA and IQ mixing matrix obtained by real ML-ICA, respectively, which is used to estimate Tx XY and IQ imbalance; $S_{OUT,X/Y}$ represents the final output signal of DSP on X/Y polarization state; $\lambda_{X/Y}$ and λ_{XY} represent IQ and XY amplitude ratio of the final output signal, respectively, which can be used to mitigate the interaction between amplitude/phase imbalance and time skew. The IQ/XY amplitude ratios are given as follows:

$$\lambda_{\boldsymbol{X}} = E(|imag(s_{OUT,X}(n)|)) / E(|real(s_{OUT,X}(n)|)) \tag{10}$$

$$\lambda_{\boldsymbol{Y}} = E(|imag(s_{OUT,Y}(n)|)) / E(|real(s_{OUT,Y}(n)|)) \tag{11}$$

$$\lambda_{\boldsymbol{XY}} = E(|(s_{OUT,X}(n)|) / E(|(s_{OUT,Y}(n)|) \tag{12}$$

To decouple multiple impairments between the Tx and Rx, the DSP flow of the proposed scheme is reversed in comparison to the order of impairments' introduction. Firstly, Rx impairments are monitored and compensated. Godard TED is used to estimate the timing error of each path of the detected signal. The timing error is further used to calculate Rx IQ/XY skews; the Rx IQ/XY amplitude imbalance and IQ phase imbalance are estimated from the statistics based on GSOP. After compensating Rx impairments, Tx impairments are monitored. A modified complex ML-ICA based on a real score function is used to obtain inverse Jones matrix and track polarization; subsequently, 4-th fast Fourier transform (FFT) is used to compensated FO [23]; real-ML-ICA is used to obtain inverse IQ mixing matrix and compensate phase noise and Tx IQ amplitude/phase imbalance; then Godard TED is used again to estimate Tx IQ/XY skews. Finally, the obtained inverse Jones/IQ mixing matrices and IQ/XY amplitude ratio of the final output signal are employed to estimate Tx IQ/XY imbalance. In this process, the IQ amplitude ratio and inverse IQ mixing matrix are used to estimate Tx IQ amplitude/phase imbalance. Then the Tx IQ amplitude imbalance, XY amplitude ratio, and inverse Jones matrix are used to estimate Tx XY amplitude.

It is noteworthy that all the algorithms can be used for arbitrary modulation format signals except 4-th FFT which can only be used for square QAM signals. Therefore, the proposed algorithm is applicable for arbitrary QAM square modulation format and has the potential to be used in arbitrary modulation format. The detailed algorithm principles are given in the following section.

C. Rx imbalance monitoring

Firstly, the Rx imbalance monitoring principle is given in absence of Tx imbalance. Godard TED is used to estimate IQ/XY skew, which can extract timing error from the autocorrelation coefficient spectrum of received signals and further calculate time skew. In this paper, the received signals are divided into several signal blocks as the input of Godard TED and the block length is set to 1024. Assuming the signal in the frequency domain can be expressed as:

$$S_{Tx/Rx,mn}(n) = FFT(s_{Tx/Rx,mn}(n)) \tag{13}$$

where n is the index of sampled signal in time/frequency domain.

According to the theory of Godard TED, the timing error of each path of received signal can be expressed as [7]:

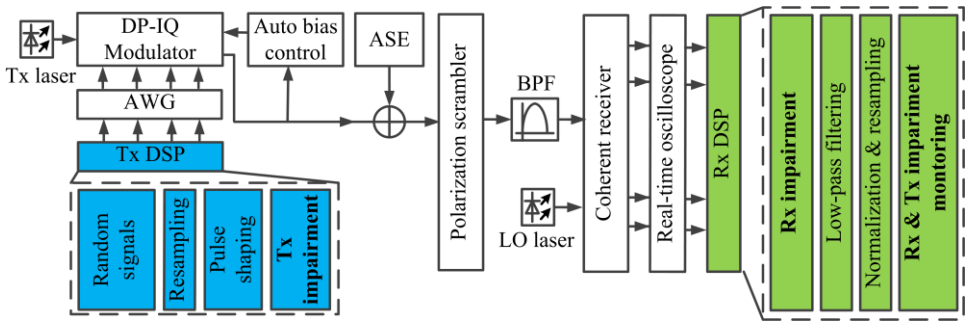

Fig. 4 System diagram.

$$t(k) = angle(\sum_{n=(k-1)*N+1}^{k*N-N/2} S_{Rx,mn}(n) S_{Rx,mn}^{*}(n+N/2)) / 2\pi f \quad (14)$$

where k is the block index, N is the FFT points and block length, f is the symbol rate. Then time skew is given that:

$$\begin{aligned} \tau_{Rx,X} &= \mathrm{E}(t_{Rx,XQ}(k) - t_{Rx,XI}(k)) \\ \tau_{Rx,Y} &= \mathrm{E}(t_{Rx,YQ}(k) - t_{Rx,YI}(k)) \\ \tau_{Rx,XY} &= \mathrm{E}(t_{Rx,YI}(k) - t_{Rx,XI}(k)) \end{aligned} \quad (15)$$

where $t_{Rx,XI}$, $t_{Rx,XQ}$, $t_{Rx,YQ}$, and $t_{Rx,YQ}$ represent the timing errors of XI, XQ, YI, and YQ path of the received signal.

In the general Rx model, the Rx amplitude/phase imbalance is introduced before time skew, as given in (8) and (9). These imbalances do not change the relative delay of IQ and XY components and will not affect time skew estimation based on Godard TED. After compensating Rx skew, Rx IQ/XY amplitude imbalance and IQ phase imbalance can be estimated from statistics of the received signal based on GSOP:

$$g_{Rx,X} = \sqrt{\mathrm{E}(s_{Rx,XI}^2(n)) / \mathrm{E}(s_{Rx,XQ}^2(n))} \quad (16)$$

$$g_{Rx,XY} = \sqrt{\mathrm{E}(s_{Rx,YI}^2(n)) / \mathrm{E}(s_{Rx,XI}^2(n))} \quad (17)$$

$$\begin{aligned} \theta_{Rx,X} &= -\arctan(\mathrm{E}(s_{Rx,XI}(n) s_{Rx,XQ}(n)) \\ &/ \sqrt{\mathrm{E}(s_{Rx,XI}^2(n))\mathrm{E}(s_{Rx,XQ}^2(n)) - \mathrm{E}^2(s_{Rx,XI}(n) s_{Rx,XQ}(n))}) \end{aligned} \quad (18)$$

where E and arctan represent the average and arctangent operation, respectively.

D. Separation of Rx and Tx imbalances

Rx and Tx imbalances will couple with each other, which makes it difficult to estimate these imbalances. To deal with this issue, the separation principle of Rx and Tx imbalances is discussed in this section.

IQ imbalance is actually the relative difference or imperfect between IQ components. Obviously, these imbalances will disappear when IQ components are totally mixed. In the heterodyne system, Tx imbalance and Rx imbalance are introduced before and after FO. Therefore, the continuous phase rotation induced by FO will conceal the Tx IQ imbalance and not change Rx IQ imbalance. Based on this, Tx IQ imbalance has no impact on Rx IQ imbalance monitoring when FO exits and the transceiver IQ imbalance separation is achieved. The detailed principle is as follows:

Firstly, the IQ skew separation is investigated. Given the phase rotation matrix caused by FO can be expressed as:

$$\boldsymbol{P}_{\boldsymbol{R}}(t) = \begin{bmatrix} \cos(\Delta\omega t) & -\sin(\Delta\omega t) \\ \sin(\Delta\omega t) & \cos(\Delta\omega t) \end{bmatrix} \quad (19)$$

$$\Delta\omega = \omega_s - \omega_{LO}$$

Assuming there is no polarization misalignment and only the skew dependent parameters and phase rotation matrix are considered, then the received signal on X polarization can be expressed as:

$$\begin{aligned} \begin{bmatrix} s'_{Rx,XI}(t) \\ s'_{Rx,XQ}(t) \end{bmatrix} &\propto \begin{bmatrix} 1 & 0 \\ 0 & \delta(t-\tau_{Rx,X}) \end{bmatrix} \otimes \begin{bmatrix} s_I(t) \\ s_Q(t) \end{bmatrix} \\ \begin{bmatrix} s_I(t) \\ s_Q(t) \end{bmatrix} &= \boldsymbol{P}_{\boldsymbol{R}}(t) \begin{bmatrix} s'_{Tx,XI}(t) \\ s'_{Tx,XQ}(t) \end{bmatrix} \\ \begin{bmatrix} s'_{Tx,XI}(t) \\ s'_{Tx,XQ}(t) \end{bmatrix} &= \begin{bmatrix} 1 & 0 \\ 0 & \delta(t_s-\tau_{Tx,X}) \end{bmatrix} \otimes \begin{bmatrix} s_{Tx,XI}(t) \\ s_{Tx,XQ}(t) \end{bmatrix} \end{aligned} \quad (20)$$

After sampling and time-frequency conversion, the received signal can be expressed as:

$$\begin{aligned} \begin{bmatrix} S'_{Rx,XI}(n) \\ S'_{Rx,XQ}(n) \end{bmatrix} &\propto \begin{bmatrix} 1 & 0 \\ 0 & \exp(-i2\pi\tau_{Rx,X} n/N) \end{bmatrix} \begin{bmatrix} S_I(n) \\ S_Q(n) \end{bmatrix} \\ \begin{bmatrix} S_I(n) \\ S_Q(n) \end{bmatrix} &= \mathcal{F}\left\{ \begin{bmatrix} \cos(\Delta\omega n T_s) & -\sin(\Delta\omega n T_s) \\ \sin(\Delta\omega n T_s) & \cos(\Delta\omega n T_s) \end{bmatrix} \right\} \otimes \begin{bmatrix} S'_{Tx,XI}(n) \\ S'_{Tx,XQ}(n) \end{bmatrix} \end{aligned} \quad (21)$$

According to (15), (20), and (21), the Rx IQ skew on X polarization can be expressed as:

$$\begin{aligned} \tau &= \mathrm{E}(t_{S'_{Rx,XI}}(k) - t_{S'_{Rx,XQ}}(k)) \\ &= \tau_{Rx,X} + \mathrm{E}(t_{S_I}(k)) - \mathrm{E}(t_{S_Q}(k)) \end{aligned} \quad (22)$$

When FO exists and data is enough, $\Delta\omega n T_s$ can satisfy the condition of traversing [0 2π] degrees. Then the following equations are valid:

$$\mathrm{E}(\cos(\Delta\omega n T_s)) = \mathrm{E}(\sin(\Delta\omega n T_s)) = 0 \quad (23)$$

$$\mathrm{E}(t_{S_I}(k)) = \mathrm{E}(t_{S_Q}(k)) = 0 \quad (24)$$

Substituting (21) into (19):

$$\tau = \tau_{Rx,X} \quad (25)$$

Therefore, Rx IQ skew monitoring is unaffected by Tx IQ skew if FO is present.

Next, the transceiver IQ amplitude/phase imbalance separation is investigated. Assuming polarization crosstalk and time skew are compensated perfectly, the received signal on X polarization can be expressed as:

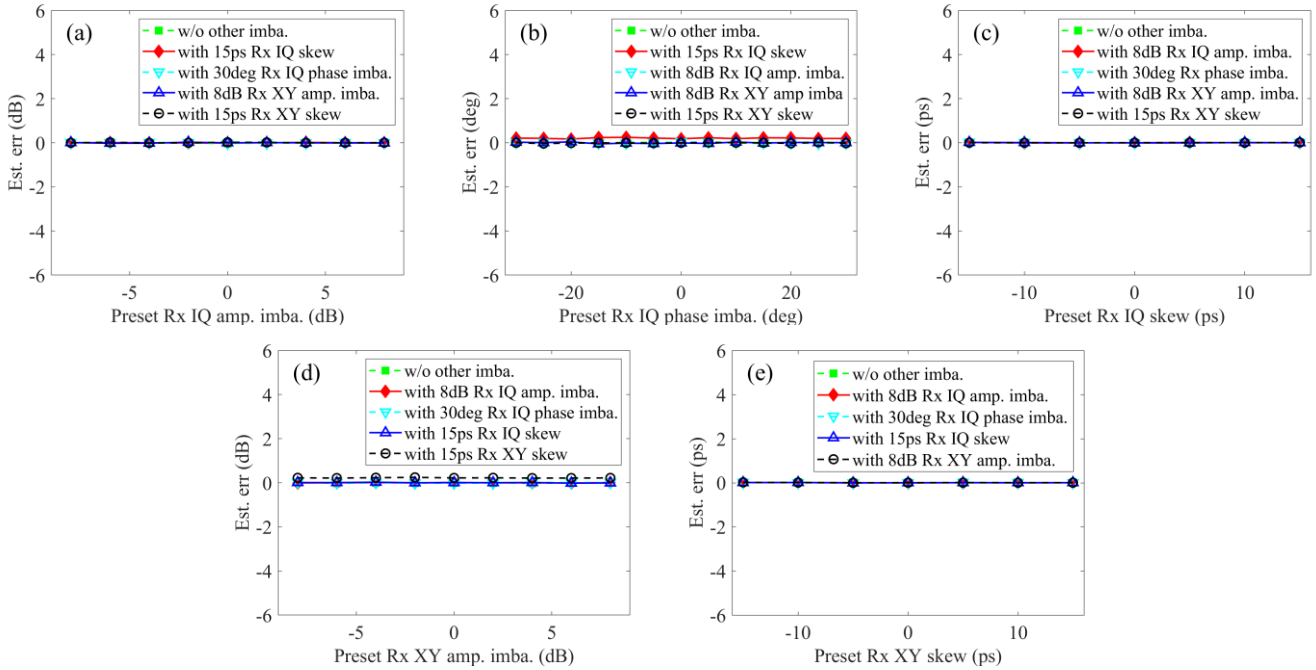

Fig. 5 Rx imbalance monitoring. (a) Rx IQ amplitude imbalance; (b) Rx IQ phase imbalance; (c) Rx IQ skew; (d) Rx XY amplitude imbalance; (e) Rx XY skew.

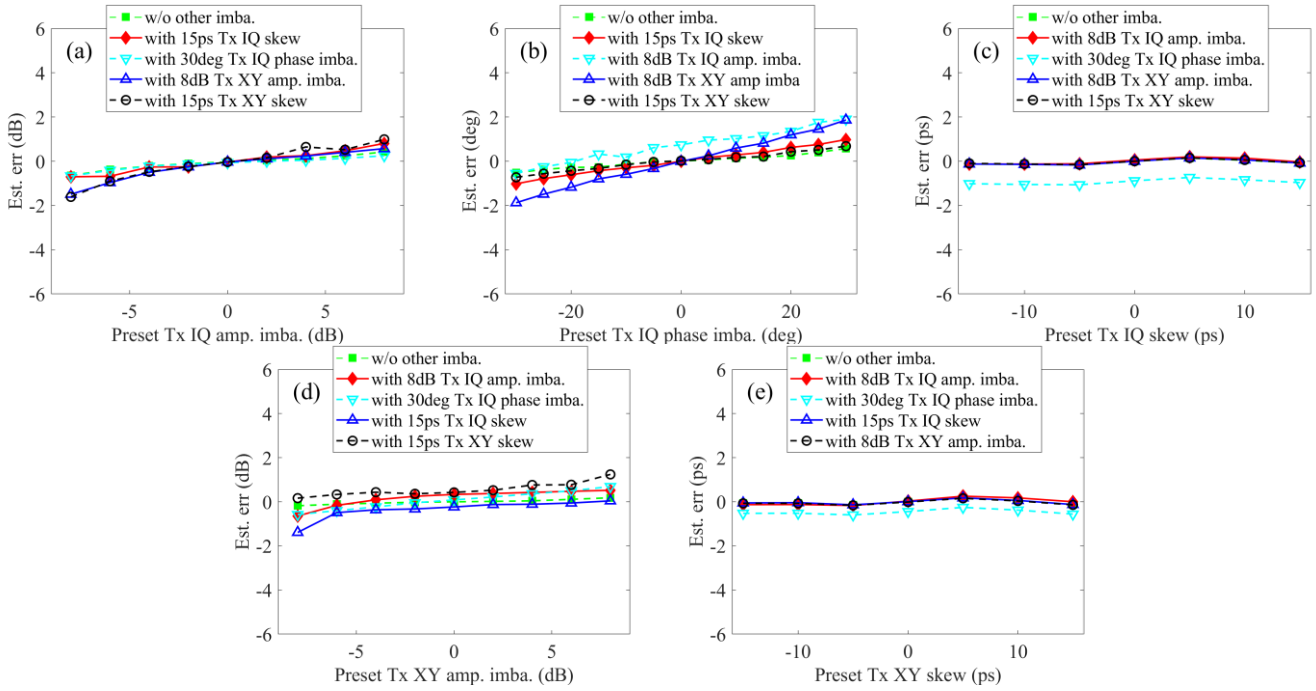

Fig. 6 Tx imbalance monitoring. (a) Tx IQ amplitude imbalance; (b) Tx IQ phase imbalance; (c) Tx IQ skew; (d) Tx XY amplitude imbalance; (e) Tx XY skew.

$$\begin{bmatrix} s'_{Rx,XI}(n) \\ s'_{Rx,XQ}(n) \end{bmatrix} \propto \begin{bmatrix} 1 & 0 \\ -g_{Rx,X}\sin(\theta_{Rx,X}) & g_{Rx,X}\cos(\theta_{Rx,X}) \end{bmatrix} \boldsymbol{P_R}(n) \bullet \begin{bmatrix} 1 & -g_{Tx,X}\sin(\theta_{Tx,X}) \\ 0 & g_{Tx,X}\cos(\theta_{Tx,X}) \end{bmatrix} \begin{bmatrix} s_{Tx,XI}(n) \\ s_{Tx,XQ}(n) \end{bmatrix} = \begin{bmatrix} 1 & 0 \\ -g_{Rx,X}\sin(\theta_{Rx,X}) & g_{Rx,X}\cos(\theta_{Rx,X}) \end{bmatrix} \begin{bmatrix} s'_I(n) \\ s'_Q(n) \end{bmatrix} \tag{26}$$

If $\Delta\omega nT_s$ traverses the interval from 0 to 2π, then:

$$\begin{aligned} E(s'^2_I(n)) &= E(s'^2_Q(n)) = \sigma^2\pi(1+g^2_{Tx,X}) \\ E(s'_I(n)s'_Q(n)) &= 0 \end{aligned} \tag{27}$$

According to (22) and (23), it can be proved that:

$$g_{Rx,X} = \sqrt{E(s'^2_{Rx,XI}(n)) / E(s'^2_{Rx,XQ}(n))} \tag{28}$$

$$\theta_{Rx,X} = -arc\tan(E(s'_{Rx,XI}(n)s'_{Rx,XQ}(n)) / \sqrt{E(s'^2_{Rx,XI}(n))E(s'^2_{Rx,XQ}(n)) - E^2(s'_{Rx,XI}(n)s'_{Rx,XQ}(n))}) \tag{29}$$

By comparing (16), (17), (28), and (29), Rx IQ

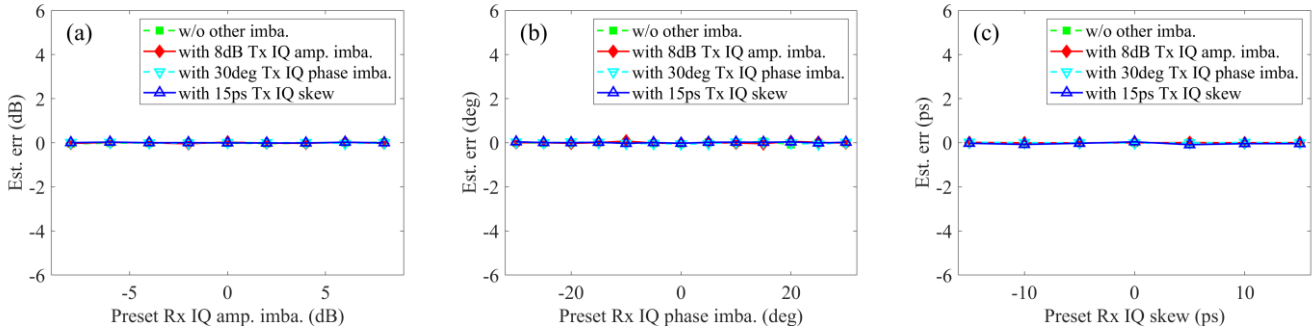

Fig. 7 Rx IQ imbalance monitoring under Tx IQ imbalance. (a) Rx IQ amplitude imbalance; (b) Rx IQ phase imbalance; (c) Rx IQ skew.

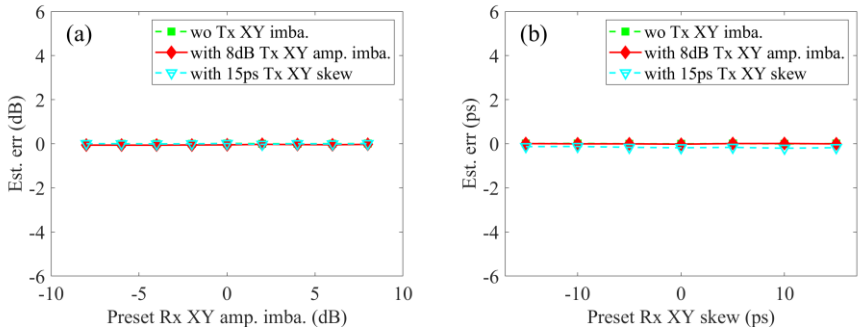

Fig. 8 Rx XY imbalance monitoring under Tx XY imbalance. (a) Rx XY amplitude imbalance; (b) Rx XY skew.

amplitude/phase imbalance estimation based on GSOP is unaffected by Tx IQ amplitude/phase imbalance in presence of FO. To sum up, if $\Delta\omega nT_s$ traverses the interval of [0 2π], transceiver IQ separation can be achieved based on FO.

XY imbalance represents the relative difference between XY components, which is somewhat similar to IQ imbalance. Considering IQ imbalance can be separated by using the continuous phase rotation, the XY imbalance also can be separated by using continuous polarization rotation. According to (15), (16), and (17), XY imbalance separation is not affected by the phase-related parameters of ξ and η. In this condition, the polarization rotation matrix $\boldsymbol{J}_{\boldsymbol{R}}$ is equivalent to phase rotation matrix $\boldsymbol{P}_{\boldsymbol{R}}$ for imbalance separation. By analogy to the IQ imbalance separation, if κ traverses [0 2π], Rx XY imbalance monitoring is independent of Tx XY imbalance before polarization tracking and thus transceiver XY imbalance separation can be achieved by using continuous polarization rotation. To save space, we will not discuss it in detail.

E. Tx imbalance monitoring

Considering Tx imbalance is introduced firstly, polarization tracking and CPR should be implemented before Tx imbalance monitoring. In our previous research, complex ML-ICA is used to track polarization. The scheme can be used to implement blind source separation by maximizing the non-gaussianity of the received signal, which has a strong tolerance for Tx impairment and does not suffer singularity problem [24]. However, the complex ML-ICA only can be used to track polarization in absence of FO, which is not applicable for the FO based transceiver IQ imbalance separation scheme. In this paper, the previous complex ML-ICA is modified by using a novel real score function and the modified algorithm is immune to FO and phase noise for polarization tracking. The real score function is derived from the sub-Gaussian probability density function and the related expression is as follow:

$$\varphi(\boldsymbol{Z}_{out}(n)) = \mathrm{sign}(\boldsymbol{Z}_{out}(n))(\tan(|\boldsymbol{Z}_{out}(n)|) - |\boldsymbol{Z}_{out}(n)|) \quad (30)$$

where $\boldsymbol{Z}_{out}(n)$ is the output signal of complex-ML-ICA and sign(.) is the sign function. Due to the normalization function of complex-ML-ICA, the obtained inverse Jones matrix can be used to estimate Tx XY amplitude imbalance (as shown in (36)). After using 4-th FFT to compensate FO, the real ML-ICA is used to compensate phase noise and the obtained inverse IQ mixing matrix is further used to estimate Tx IQ amplitude/phase imbalance. Finally, the Godard TED is used to estimate Tx IQ/XY skew, which is the same as Rx skew monitoring. It is noteworthy that the power change caused by time skew will induce additional amplitude imbalance. Therefore, the IQ/XY amplitude ratio of final output signal should be fed back to eliminate the interaction of time skew and IQ/XY imbalance.

Given the obtained inverse Jones matrix obtained $\boldsymbol{M}$ and inverse IQ mixing matrix $\boldsymbol{B}$ are expressed as：

$$\boldsymbol{M} = \begin{bmatrix} M_{xx} & M_{xy} \\ M_{yx} & M_{yy} \end{bmatrix} \quad (31)$$

$$\boldsymbol{B} = \begin{bmatrix} B_{II} & B_{IQ} \\ B_{QI} & B_{QQ} \end{bmatrix} \quad (32)$$

Then the Tx IQ amplitude/phase imbalance can be estimated by using $\lambda_{X/Y}$ and $\boldsymbol{B}$:

$$\psi_{X/Y} = -\arctan(B_{QI} / B_{QQ}) \quad (33)$$

$$\alpha_{X/Y} = 1/(B_{II}\cos(\psi) + \lambda_{X/Y} B_{IQ}\sin(\psi)) \quad (34)$$

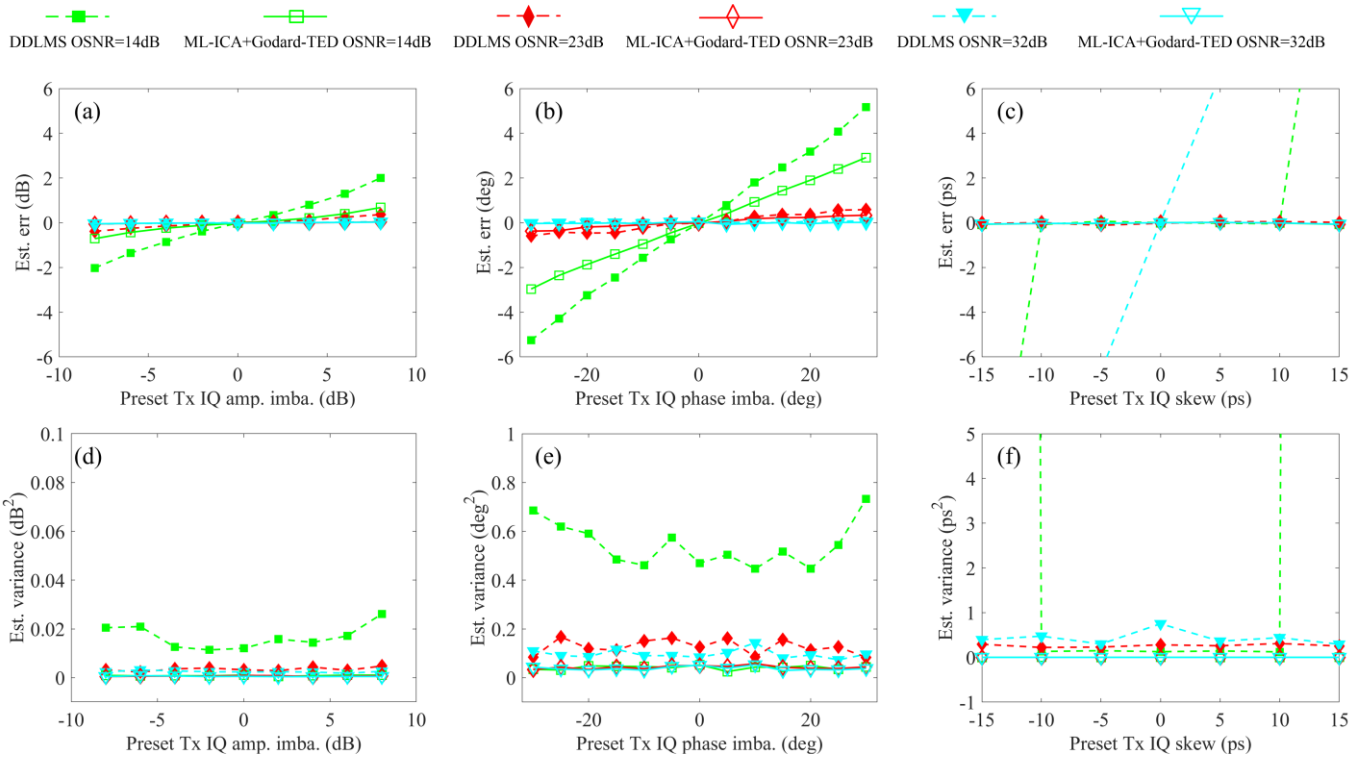

Fig. 9. ASE noise tolerance of Tx IQ imbalance monitoring algorithm characterized by estimation error and variance. (a) and (d) Tx IQ amplitude imbalance estimation error and variance; (b) and (e) Tx IQ phase imbalance estimation error and variance; (c) and (f) Tx IQ skew estimation error and variance.

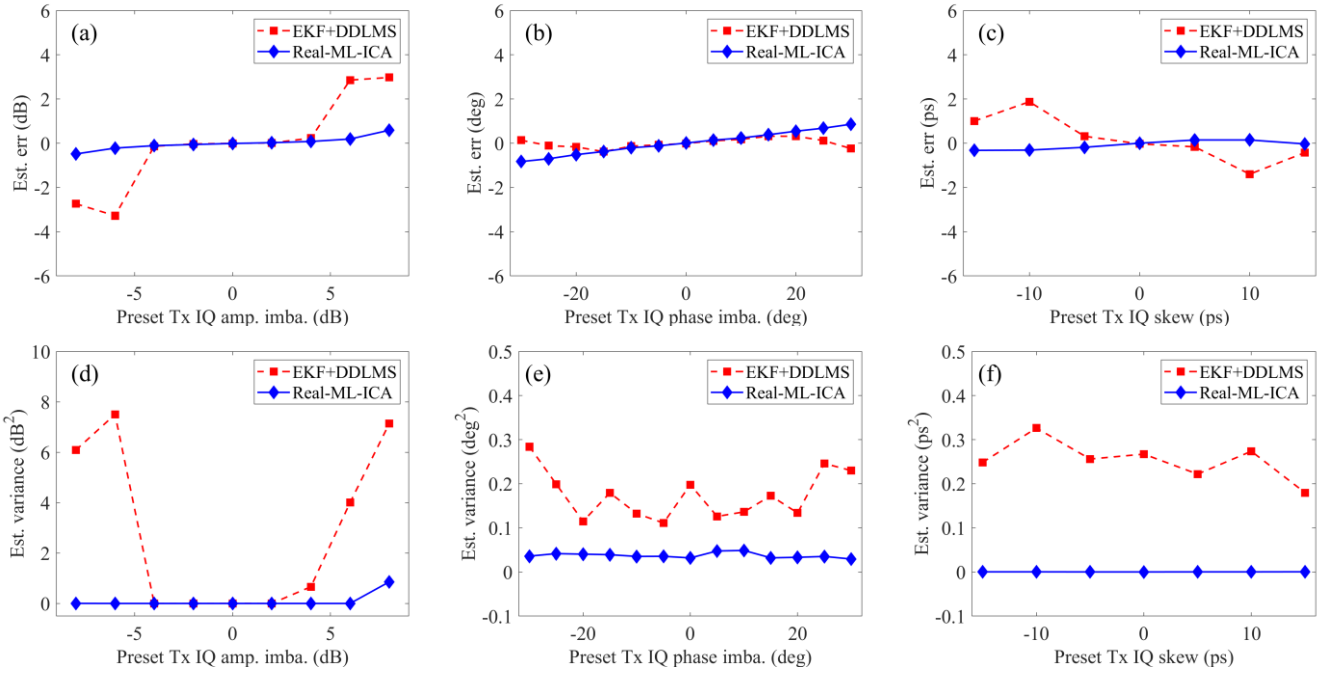

Fig. 10. Tx IQ imbalance tolerance of CPR algorithm characterized by estimation error and variance. (a) and (d) Tx IQ amplitude imbalance estimation error and variance; (b) and (e) Tx IQ phase imbalance estimation error and variance; (c) and (f) Tx IQ skew estimation error and variance.

$$\theta_{Tx,X/Y} = \arctan((-B_{II}\sin(\psi)+B_{IQ}\cos(\psi)) /(B_{II}\cos(\psi)+B_{IQ}\sin(\psi))) \tag{35}$$

$$g_{Tx,X/Y} = \lambda_{X/Y} / (-\alpha\sin(\theta)(B_{QI}\cos(\psi)+B_{QQ}\sin(\psi)) +\alpha\cos(\theta)(-B_{QI}\sin(\psi)+B_{QQ}\cos(\psi))) \tag{36}$$

The XY amplitude imbalance can be estimated by using λ_{XY} and $\boldsymbol{M}$:

$$g_{Tx,XY} = E(\sqrt{(M_{XX}^2+M_{XY}^2)/M_{YX}^2+M_{YY}^2}) \bullet\lambda_{XY}\sqrt{(1+g_{Tx,X}^2)/(1+g_{Tx,Y}^2)} \tag{37}$$

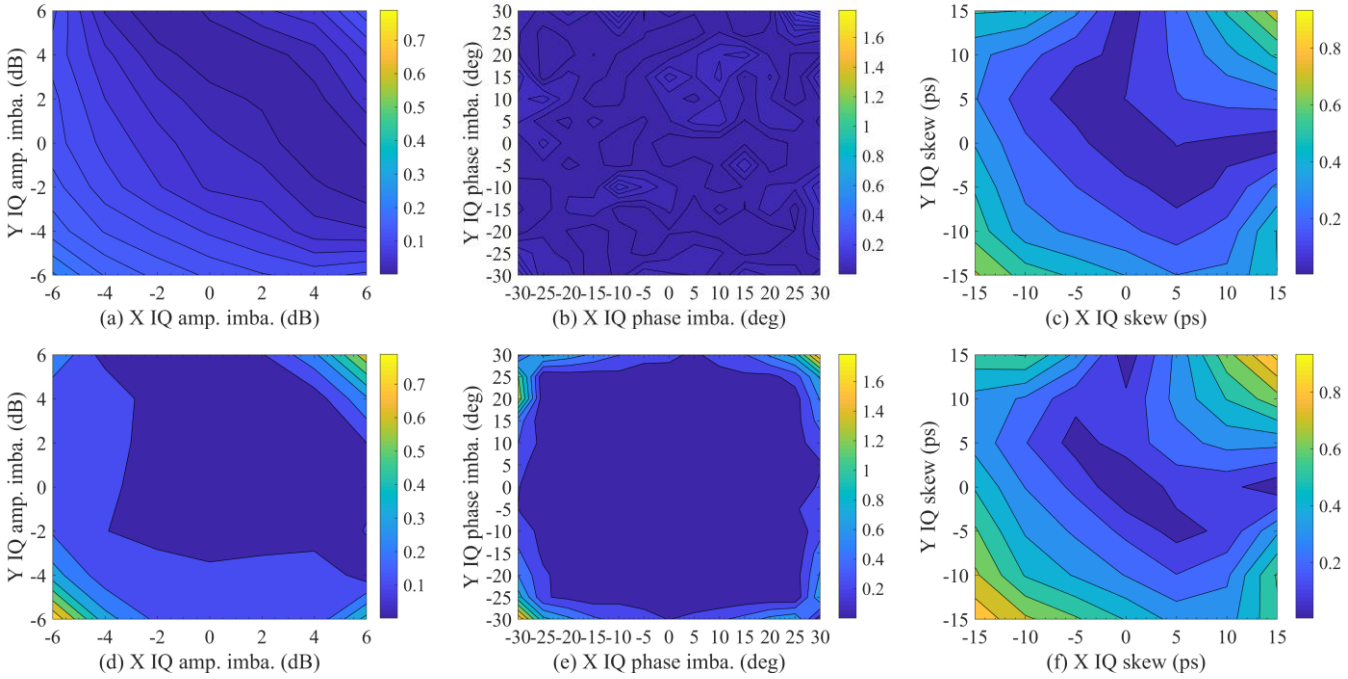

Fig. 11 Tx IQ imbalance tolerance of polarization tracking algorithm characterized by estimation error. (a)-(c) Complex-ML-ICA+real-ICA; (d)-(f) Complex-RDE+real-ICA; (a) and (d) Tx IQ amplitude imbalance monitoring; (b) and (e) Tx IQ phase imbalance monitoring; (c)-(f) Tx IQ skew monitoring.

III. Numerical Simulation

In this section, the influence of imbalance interaction on the proposed scheme is discussed firstly to investigate the imbalance separation performance. Subsequently, the proposed scheme is compared with DDLMS/RDE+EKF to investigate the monitoring range. The schematic diagram of 28 Gbaud PDM-16QAM system model is shown in Fig. 4. The laser linewidth is set to 100 KHz, and the polarization rotation rate of the scrambler is set to 1 MHz. The OSNR is set to 23 dB by default. The root raised cosine (RRC) filter is used to implement pulse shape and roll-off is set to 1. The estimation errors are obtained from the average of 10 independent trials and 2^{16} symbols are used. In order to keep consistent with the following experimental section, the transceiver imbalances are digitally added in the DSP model of Rx and Tx. The related imbalances include: Rx/Tx IQ amplitude/phase imbalance and skew; Rx/Tx XY amplitude imbalance and skew.

A. *Rx imbalance interaction*

Firstly, the influence of Rx imbalance interaction on Rx imbalance monitoring is discussed. The monitoring performance of single Rx imbalance is compared with that of joint Rx imbalance. The single imbalance monitoring is to monitor only one kind of targeted imbalance and related to the result "without other imbalance" in Fig. 5. The joint imbalance monitoring is to monitor the targeted imbalances jointly when multiple imbalances co-exist and related to the result "with imbalance" in Fig .5. The estimation error of joint imbalance is close to that of single Rx imbalance monitoring and any other Rx imbalance has no impact on the current Rx imbalance monitoring, as shown in Fig. 5. Therefore, the accuracy of the proposed scheme is not affected by Rx imbalance interaction and the proposed scheme can achieve joint Rx imbalance monitoring.

B. *Tx imbalance interaction*

Next, the influence of Tx imbalance interaction on Tx imbalance monitoring is discussed. The related Tx imbalance is monitored when the single/joint imbalance exists. As shown in Fig. 6, the estimation error of target imbalance increases marginally with another Tx imbalance, even if both these imbalances have a large magnitude. Therefore, the proposed scheme still shows strong robustness to Tx imbalance interaction and achieve joint Tx imbalance monitoring. Besides, the estimation error of Tx imbalance is slightly larger than that of Rx imbalance, which is mainly caused by the performance degradation of polarization tracking and CPR.

C. *Transceiver imbalance interaction*

Transceiver imbalance interaction involves transceiver IQ and XY imbalance interaction. The proposed scheme utilizes the FO naturally existing in the system and continuous polarization rotation induced by polarization scrambler to achieve transceiver IQ and XY imbalance separation, respectively. As shown in Fig. 7 and 8, the proposed scheme can accurately estimate Rx IQ/XY imbalance under Tx IQ/XY imbalance. This means that the estimation of Rx imbalance is unaffected by the Tx imbalance. Based on this, the proposed scheme can achieve accurate Rx IQ/XY imbalance monitoring before FO compensation/polarization tracking. Consequently, the transceiver imbalance separation is achieved successfully.

D. *The factors affecting the monitoring range*

In addition to imbalance separation, the difficulty of transceiver imbalance monitoring is how to improve the

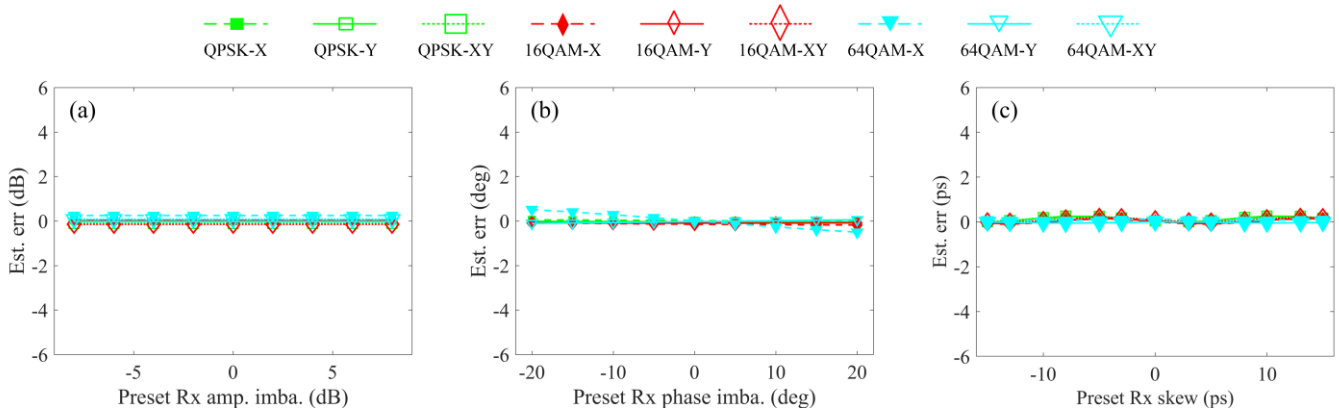

Fig. 12 Experiment of Rx imbalance monitoring. (a) Amplitude imbalance; (b) phase imbalance; (c) time skew.

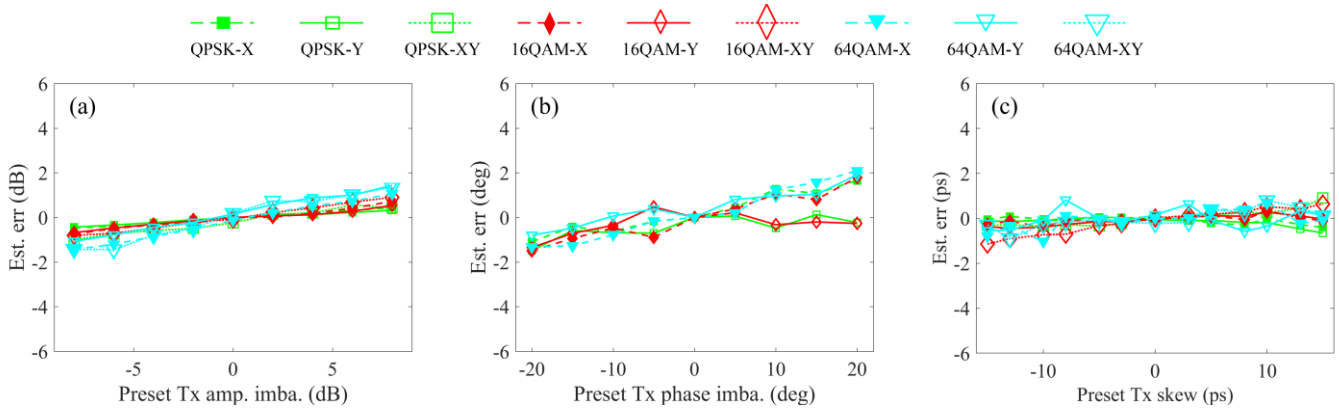

Fig. 13 Experiment of Tx imbalance monitoring. (a) Amplitude imbalance; (b) phase imbalance; (c) time skew.

monitoring range of Tx imbalance. Compared with Rx imbalance, Tx imbalance is introduced firstly and vulnerable to ASE noise, polarization crosstalk, and phase noise. Therefore, the monitoring range of Tx imbalance is determined by the ASE noise/Tx imbalance tolerance of the Tx imbalance estimation/CPR and polarization tracking algorithms. Considering that the ultimate purpose of transceiver imbalance monitoring is to monitor transceiver imbalance, the tolerance of each algorithm module for different signal impairments is reflected by the imbalance monitoring error in the following simulation. The comparison of Rx imbalances monitoring is not discussed in this paper, because the conventional algorithm, such as GSOP and Godard-TED, are used in the proposed scheme. Besides, Tx XY imbalances are also not considered for the reason that the conventional algorithm can not monitor these imbalances.

E. The ASE noise tolerance of Tx imbalance estimation

Firstly, the ASE noise tolerance of Tx imbalance estimation is investigated. Assuming Rx imbalance, polarization crosstalk, FO, and phase noise are compensated ideally, only Tx IQ imbalances are considered. In conventional scheme, the real-DDLMS algorithm is used to estimate the Tx IQ amplitude/phase imbalance and skew jointly. In the proposed scheme, real-ML-ICA/Godard-TED is used to estimate Tx IQ amplitude and phase imbalance/skew.

As shown in Fig. 9, the real-ML-ICA+Godard-TED algorithm of the proposed scheme is compared with real-DDLMS under different OSNR conditions. For the Tx IQ amplitude/phase imbalance monitoring, the real-DDLMS algorithm has a larger monitoring error compared with real-ML-ICA algorithm under the low OSNR conditions. These results can be attributed to the fact that real-DDLMS will suffer more decision errors at low SNR. However, real-ML-ICA does not need to make signal decision and avoids such decision errors, and thus can tolerate more ASE noise. For the Tx IQ skew monitoring, Godard-TED algorithm achieves sufficient accuracy within a wide Tx IQ imbalance range under different OSNR condition. However, real-DDLMS algorithm will fail to work at low or high OSNR. This performance comparison result can be explained as follows: under low OSNR condition, real-DDLMS suffers serious decision error, but Godard-TED avoids such decision error due to its decision free operation; under high OSNR condition, DDLMS equalizer will amplify high-frequency noise considering the signal spectrum is non-flat in this simulation and these noises will degrade the monitoring accuracy of time skew. However, Godard-TED does not equalize the channel, which will not induce extra high-frequency noise. It is noteworthy that real-DDLMS can achieve accurate time skew monitoring by using special pulse shaping or pre-emphasis filter to make the signal spectrum flat, which undoubtedly reduces the system flexibility. In addition, the estimation variance of real-ML-ICA+Godard-TED is less than that of real-DDLMS in these comparisons. Therefore, the proposed scheme has a stronger tolerance to ASE noise compared with real-DDLMS for Tx IQ imbalance monitoring

TABLE I
JOINT TRANSCEIVER IMBALANCE MONITORING

Device	Polarization	Imbalance	Preset value	Estimation value/mean error		
				QPSK	16QAM	64QAM
Rx	X	Amp. imba. (dB)	1	1.10±0.14 /-0.10	1.16±0.13 /-0.16	0.89±0.28 /0.11
		Phase imba. (deg)	6	5.84±0.15 /0.16	5.92±0.17 /0.08	5.85±0.13 / 0.15
		Skew (ps)	5	4.92±0.26 /0.08	5.04±0.28 /-0.04	5.20±0.62 /-0.20
	Y	Amp. imba. (dB)	-3	-3.07±0.11 /0.07	-3.03±0.13 /0.03	-3.03±0.32 /0.03
		Phase imba. (deg)	-8	-7.87±0.15 /-0.13	-7.87±0.16 /-0.13	-7.87±0.15 /-0.13
		Skew (ps)	-4	-3.88±0.21 /-0.12	-3.96±0.22 /-0.04	-4.24±0.45 /0.24
	XY	Amp. imba. (dB)	2	2.20±0.08 /-0.2	2.20±0.10 /-0.20	1.78±0.34 /0.22
		Skew (ps)	7	6.50±0.65 /0.50	6.69±0.63 /0.31	6.75±0.88 /0.25
Tx	X	Amp. imba. (dB)	1	1.28±0.05 /-0.28	1.27±0.06 /-0.27	0.97±0.21 /0.03
		Phase imba. (deg)	6	5.64±0.50 /0.36	7.10±0.47 /1.10	5.98±1.23 /0.02
		Skew (ps)	5	4.96±0.12 /0.04	4.80±0.12 /0.20	5.47±0.65 /-0.47
	Y	Amp. imba. (dB)	-3	-2.62±0.04 /-0.38	-2.57±0.07 /-0.43	-3.03±0.30 /0.03
		Phase imba. (deg)	-8	-7.22±0.69 /-0.78	-7.35±0.99 /-0.65	-7.07±0.21 /-0.93
		Skew (ps)	-4	-4.07±0.10 /0.07	-3.86±0.09 /-0.14	-4.42±0.52 /0.42
	XY	Amp. imba. (dB)	2	1.67±0.11 /0.33	1.66±0.10 /0.34	1.69±0.32 /0.31
		Skew (ps)	7	6.94±0.22 /0.06	6.64±0.18 /0.36	7.53±0.81 /-0.53

and thus has a wider monitoring range under extreme OSNR conditions.

F. The Tx IQ imbalance tolerance of CPR and polarization tracking algorithm

Next, the IQ imbalance tolerances of CPR and polarization tracking algorithm are investigated, respectively. The EKF/complex-RDE and real/complex-ML-ICA algorithms are used in the conventional scheme and proposed scheme to implement CPR/polarization tracking.

To verify the Tx IQ imbalance-tolerance of CPR algorithm, the real-ML-ICA of the proposed scheme is compared with EKF+real-DDLMS algorithm. In this simulation, only phase noise and Tx IQ imbalance are considered and OSNR is set to 23 dB to ensure that only the CPR performance difference exists. As shown in Fig. 10, the simulation demonstrates real-ML-ICA has a smaller estimation error and variance compared with EKF+real-DDLMS when the imbalances are serious. Therefore, real-ML-ICA is more tolerable to Tx IQ amplitude imbalance and skew compared with EKF for CPR.

To test the Tx imbalance-robustness of polarization tracking algorithm, the complex-ML-ICA+real-ML-ICA of the proposed scheme is compared with complex-RDE+real-ML-ICA. In these two schemes, the complex-ML-ICA/complex-RDE is used to tracking polarization and real-ML-ICA is used to implement CPR. These algorithm configurations can ensure that only the difference of polarization tracking performance exists in the simulation. As shown in Fig. 11, the simulation results demonstrate the complex-ML-ICA is more robust to Tx IQ imbalance compared with complex-RDE for polarization tracking.

The above simulation results on the Tx IQ imbalance-tolerance of CPR and polarization tracking can be explained as follows: the convergence principle of EKF and RDE is to minimize the constellation decision error between the received signal and related ideal signal. However, Tx imbalances distort the signal constellation, which may increase the constellation decision error and causes these algorithms fail to converge. Therefore, the conventional algorithms based on the constellation decision are sensitive to Tx imbalance. However, the convergence principle of ICA is maximizing the non-gaussianity and is independent of the decision error of signal constellation. To sum up, the proposed scheme can achieve more reliable polarization tracking and CPR in presence of Tx imbalance, which indirectly increases the monitoring range.

IV. EXPERIMENTAL SETUP AND RESULT

In order to verify the modulation-format-transparency and

multi-dimension monitoring, the proposed scheme is tested in the experimental system. The experimental setup is the same as the above numerical simulation, where the type of polarization scrambler is agiltron NOPS-11511133 and the maximum polarization rotation speed is 5 MHz, other experimental devices can refer to [10]. To demonstrate the modulation-format-transparency, 28 Gbaud PDM-QPSK/16QAM/64QAM signals are used and the same parameters are set in the proposed scheme for different modulation formats. The experimental results are obtained by the average of 10 independent trials and 10^6 sampling signals are used in each trial.

Firstly, the proposed scheme is tested in presence of only one kind of imbalance. The experimental results show that the proposed scheme can accurately estimate each kind of transceiver imbalance for different modulation formats. With the increase of modulation format order, the monitoring errors are always kept at a low level. Therefore, the proposed scheme is modulation-format-transparent. It is noteworthy that the estimation error of Tx imbalance is slightly larger than that of Rx imbalance due to the interference of polarization crosstalk and phase noise. For Rx imbalance, the monitoring range of amplitude imbalance is [-8 8] dB within 0.2 dB error; the monitoring range of phase imbalance is [-20 20] degrees within 1-degree error; the monitoring range of time skew is [-15 15] ps within 1 ps error, as shown in Fig. 12. For Tx imbalance, the monitoring range of amplitude imbalance is [-8 8] dB within 1.5 dB error; the monitoring range of phase imbalance is [-20 20] degrees within 2-degree error; the monitoring range of time skew is [-15 15] ps within 1 ps error, as shown in Fig. 13.

Next, the proposed scheme is investigated under co-existing imbalances to verify the multi-dimensional monitoring performance. Sixteen kinds of imbalances are simultaneously added to the experimental system in Rx and Tx DPS modules. The preset/estimation values of transceiver imbalances are shown in TABLE I. The experimental results demonstrate that the proposed scheme can accurately estimate each kind of imbalance even when these imbalances co-exist. The estimation error is not changed obviously with different modulation formats, which is consistent with the conclusion of modulation-format-transparency of the previous experiment. Therefore, the proposed scheme achieves multi-dimensional transceiver imbalance monitoring in a modulation-format-transparent manner. Among these results, the estimation error of Tx imbalance is larger than Rx imbalance due to the coupling of polarization crosstalk, phase noise, and Tx imbalance. Besides, the estimation error of XY imbalance is slightly larger than that of IQ imbalance due to the insufficient polarization rotation rate or sampling points. The error can be decreased by increasing polarization rotation rate or sampling points to ensure that the received signals traverse as many polarization states as possible.

V. Conclusion

We proposed and experimentally demonstrated a novel DP-transceiver imbalance monitoring scheme for the coherent optical communication system using square-QAM signals. The scheme consists of two parts of hardware configuration and DSP module. In the hardware configuration, a polarization scrambler is set between Tx and Rx. In the DSP module, Rx and Tx imbalances are separated and monitored respectively. For the Rx imbalances, Godard-TED is employed to estimate Rx IQ/XY skew; then GSOP is used to estimate Rx IQ amplitude/phase imbalance and XY amplitude imbalance. For the Tx imbalances, the modified complex ML-ICA is firstly used to obtain inverse Jones matrix and track the polarization; after compensating FO, the real ML-ICA is used to obtain inverse IQ mixed matrix and implement CPR and Tx IQ amplitude/phase imbalance compensation; Then Godard TED is used to estimate Tx IQ/XY skew. Finally, the IQ/XY amplitude ratio of the final output signal and obtained inverse IQ mixing/Jones matrix is used to estimate the Tx IQ amplitude/phase imbalance and XY amplitude imbalance.

By utilizing the FO naturally existing in the system and continuous polarization rotation induced by polarization scrambler, the scheme achieves the separation of transceiver IQ and XY imbalance for the first time. The novel imbalance separation method together with reverse algorithm design and amplitude ratio feedback mechanism result in the proposed scheme achieving imbalance monitoring with the highest dimensionality by far. The introduction of ML-ICA which is insensitive to ASE noise/Tx imbalance gives the proposed scheme a wide monitoring range. Besides, the devices and algorithms involved in the proposed scheme are naturally independent of the modulation format. Thus the proposed scheme gives a systematic solution for modulation-format-transparent transceiver imbalance monitoring.

The simulation results demonstrate that the proposed scheme can separate and monitoring transceiver imbalance within a wide range due to the robustness to ASE noise and Tx imbalance. The experimental results confirm that the proposed scheme can achieve multi-dimensional imbalance monitoring in a modulation-format-transparent manner. In the PDM-QPSK/16QAM/64QAM experiment, the proposed scheme can estimate [- 8 8] dB amplitude imbalance within 1.5 dB error, [-20 20] degrees phase imbalance within 2 degrees error, and [-15 15] ps time skew within 1 ps error. Therefore, the proposed scheme has significant potential to be applied in high capacity and dynamic optical communication networks for comprehensive performance monitoring or module diagnosis.

References

[1] T. H. Nguyen, P. Scalart, M. Gay, L. Bramerie, C. Peucheret, T. Nguyen, M. Gautier, O. Sentieys, J. C. Simon, and M. Joindot, "Blind adaptive transmitter IQ imbalance compensation in M-QAM optical coherent systems," *IEEE/OSA J. Opt. Commun. Netw.*, vol. 9, no. 9, pp. D42-D50, Sept. 2017.

[2] Y. Yue, B. Zhang, Q. Wang, R. Lofland, J. O'Neil, and J. Anderson, "Detection and alignment of dual-polarization optical quadrature amplitude transmitter IQ and XY skews using reconfigurable interference," *Opt. express*, vol. 24, no. 6, pp. 6719-6734, Mar 2016.

[3] M. S. Faruk and K. Kikuchi, "Compensation for in-phase/quadrature imbalance in coherent-receiver front end for optical quadrature amplitude modulation," *IEEE Photonics J.*, vol. 5, no. 2, pp. 7800110, April 2013.

[4] I. Fatadin, S. J. Savory, and D. Ives, "Compensation of quadrature imbalance in an optical QPSK coherent receiver," *IEEE Photon. Technol. Lett.*, vol. 20, no. 20, pp. 1733-1735, Oct. 2008.

[5] S. J. Savory, "Digital coherent optical receivers: Algorithms and subsystems," *IEEE J. Sel. Top. Quant.*, vol. 16, no. 5, pp. 1164-1179, Oct.

2010.
[6] P. Skvortcov, C. Sanchez-Costa, I. Phillips, and W. Forysiak, “Receiver DSP Highly Tolerant to Transmitter IQ Impairments,” in *Proc. Opt. Fiber Commun. Conf.*, San Diego, USA 2019, pp. 1–3.
[7] J. Liang, Y. Fan, Z. Tao, X. Su, H. Nakashima, “Transceiver Imbalances Compensation and Monitoring by Receiver DSP,” *J. Lightwave Technol.*, early access, Oct 2019.
[8] Y. Li, M. Li, J. Han, and T. Han, “Investigation of quadrature imbalance compensation algorithm for coherent 6PolSK-QPSK,” *Phys. Commun.*, vol. 25, no. 2, pp. 319-322, Dec. 2017.
[9] N. Stojanovic and C. Xie, “An efficient method for skew estimation and compensation in coherent receivers,” *IEEE Photon. Technol. Lett.*,vol. 28, no. 4, pp. 489-492, Feb. 2015.
[10] M. Oerder and H. Meyr, “Digital filter and square timing recovery,” *IEEE T. Commun.*, vol. 36, no. 5, pp. 605-612, May 1988.
[11] M. Paskov, D. Lavery, and S. J. Savory, “Blind Equalization of Receiver In-Phase/Quadrature Skew in the Presence of Nyquist Filtering,” *IEEE Photon. Technol. Lett.*, vol. 25, no. 24, pp. 2446-2449, Dec. 2013.
[12] E. P. da Silva and D. Zibar, “Widely linear equalization for IQ imbalance and skew compensation in optical coherent receivers,” *J. Lightwave Technol.*, vol. 34, no. 14, pp. 3577-3586, Aug. 2016.
[13] C. R. S. Fludger and T. Kupfer, “Transmitter impairment mitigation and monitoring for high baud-rate, high order modulation systems,” in *Proc. Eur. Conf. Opt. Commun.*, Dusseldorf, Germany, 2016, pp. 256–258.
[14] Y. Fan, X. Su, H. Chen, J. Liang, Z. Tao, H. Nakashima, and T. Hoshlda, “Experimental verification of IQ imbalance monitor for high-order modulated transceivers,” in *Proc. Eur. Conf. Opt. Commun.*, Rome, Italy 2018.
[15] J. Diniz, F. Da Ros, E. Da Silva, R. Jones, and D. Zibar, “Optimization of DP-MQAM transmitter using cooperative coevolutionary genetic algorithm,” *J. Lightwave Technol.*, vol 36, no. 12, pp. 2450–2462, Mar. 2018.
[16] Q. Zhang, Y. Yang, C. Guo, X. Zhou, Y. Yao, A. P. T. Lau, and C. Lu, “Modulation-format-transparent IQ imbalance estimation of dual-polarization optical transmitter based on maximum likelihood independent component analysis,” *Opt. express*, vol. 27, no. 13, pp. 18055-18068, June 2019.
[17] Q. Zhang, Y. Yang, C. Guo, X. Zhou, Y. Yao, A. P. T. Lau, and C. Lu, “Algorithms for blind separation and estimation of transmitter and receiver IQ Imbalances,” *J. Lightwave Technol.*, vol. 37, no. 10, pp. 2201-2208, May 2019.
[18] C. Ju, N. Liu, and C. Li, “In-service blind transceiver IQ imbalance and skew monitoring in long-haul non-dispersion managed coherent optical systems,” *IEEE Access*, vol. 7, pp. 150051-150059, Oct. 2019.
[19] J. Liang, Y. Fan, Z. Tao, X. Su, and H. Nakashima, “Transceiver imbalances compensation and monitoring by receiver DSP,” *J. Lightwave Technol.*, Early access, Oct. 2019.
[20] P. Skvortcov, C. Sanchez-Costa, I. Phillips, and W. Forysiak, “Joint Tx and Rx skew calibration in coherent transceivers based on Rx-side DSP,” in *Proc. IEEE Photonics Conf.*, Reston, VA, USA, 2018, pp. 4-8.
[21] T. Nguyen-Ti, M. Gautier, P. Scalart, O. Berder, T. H. Nguyen, and F. A. Aoudia, “Blind I/Q imbalance compensation for *m*-QAM optical coherent systems based on pseudo-rotation,” in *Proc. Global IEEE Comm. Conf.*, Washington, DC, USA, 2016.
[22] N. Cui, X. Zhang, Z. Zheng, H. Xu, W. Zhang, X. Tang, L. Xi, Y. Fang, and L. Li, “Two-parameter-SOP and three-parameter-RSOP fiber channels: problem and solution for polarization demultiplexing using Stokes space,” *Opt. express*, vol. 26, no. 16, pp. 21170-21183, Aug. 2018.
[23] M. Selmi, Y. Jaouen, and P. Ciblat, “Accurate digital frequency offset estimator for coherent PolMux QAM transmission systems,” in *Proc. Eur. Conf. Opt. Communs.*, Vienna, Austria, 2009.
[24] P. Johannisson, H. Wymeersch, M. Sjödin, A. Tan, E. Agrell, P. Andrekson, and M. Karlsson, “Convergence comparison of the CMA and ICA for blind polarization demultiplexing,” *IEEE/OSA J. Opt. Commun. Netw.*, vol. 3, no. 6, pp. 493-501, May 2011.